# Magnetic $g$ factor of electrons in GaAs/$Al_xGa_{1-x}As$ quantum wells

M. J. Snelling, G. P. Flinn, A. S. Plaut,* R. T. Harley, and A. C. Tropper
*Physics Department, Southampton University, United Kingdom*

R. Eccleston† and C. C. Phillips
*Physics Department, Imperial College, London, United Kingdom*
(Received 10 June 1991)

The magnitude and sign of the effective magnetic splitting factor $g^*$ for conduction electrons in GaAs/$Al_xGa_{1-x}As$ quantum wells have been determined as a function of well width down to 5 nm. The experimental method is based on combined measurements of the decay time of photoluminescence and of the suppression of its circular polarization under polarized optical pumping in a magnetic field perpendicular to the growth axis (Hanle effect). Measurements as a function of hole sheet density in the wells reveal a transition from excitonic behavior with very small apparent $g$ value for low density, to larger absolute values characteristic of free electrons at higher densities. For 20-nm wells $g^*$ for electrons is close to the bulk value ($-0.44$), and increases for narrower wells passing through zero for well width close to 5.5 nm. A theoretical analysis based on three-band $\mathbf{k}\cdot\mathbf{p}$ theory, including allowance for conduction-band nonparabolicity and for wave-function penetration into the barriers, gives a reasonable representation of the data, leading to the conclusion that $g^*$ in quantum wells has a value close to that of electrons in the bulk at the confinement energy above the band minimum.

## I. INTRODUCTION

The effective magnetic splitting factor $g^*$ of conduction electrons in low-dimensional semiconductor systems is of interest for various reasons. For example, measurements can provide a test of band theory for confined electrons on a par with that given by the effective mass,[1,2] it is an important parameter for interpretation of integral and fractional quantum Hall effects, and it is also important in phenomena involving electron-nuclear spin coupling, such as optical detection of nuclear magnetic resonance.[3]

We describe here a determination of $g^*$ in type-I GaAs/$Al_xGa_{1-x}As$ quantum wells between 5 and 20 nm in width.[4] This study in these systems reveals that $g^*$ varies markedly, passing through zero for well width $L_z = 5.5$ nm. The variation is described approximately by a three-band $\mathbf{k}\cdot\mathbf{p}$ theory, including allowance for nonparabolicity of the bulk GaAs conduction band[5] and for penetration of the electronic wave-functions into the $Al_xGa_{1-x}As$ barriers. The method is based on combined measurements of the decay time of photoluminescence and of the suppression in a magnetic field of its circular polarization under polarized optical pumping (Hanle effect). The same technique has been used by Chadi, Clark, and Burnham[6] for bulk $Al_xGa_{1-x}As$ alloys.

The most precise values of $g^*$ in seminconductors are obtained using electron-spin resonance (ESR). Optically detected ESR has been applied successfully to type-II GaAs/AlAs quantum wells,[7] but works only in exceptional cases[8] for type-I systems because generally the electron lifetimes are too short.[9] Dobers, von Klitzing, and Weimann[10] have used electrically detected ESR to obtain $g^*$ in degenerate $n$-type heterojunctions and wide quantum wells. They were able to vary the "confinement" energy over a limited range by application of magnetic fields to the electron Fermi sea and obtained results in GaAs/$Al_xGa_{1-x}As$ which are in agreement with ours. More recently Krapf *et al.*[11] have reported optically detected ESR in $p$-type GaAs/$Al_xGa_{1-x}As$ heterojunctions. Their results are not directly comparable with ours as the electrons in such a system are not quantum confined and have essentially three-dimensional behavior. Determinations of spin splittings from observations of magnetoquantum oscillations in degenerate $n$-type systems are dominated by many-body exchange enhancements and do not give reliable values of the bare electron $g^*$.[12] Thus, while less precise than ESR, the present method does give useful results for type-I quantum wells and, as described below, can also determine the sign of $g^*$.

## II. EXPERIMENT

### A. Principles of the method

In a degenerate $p$-type direct-gap semiconductor, optical excitation at the absorption edge with cw circularly polarized light gives a photoexcited population of spin-polarized conduction electrons quantized with respect to the exciting beam. The spin-polarization of the holes due to photoexcitation is negligible since the photoexcited population is in general small compared to the ambient population, and their spins will in any case undergo rapid thermalization. The degree of circular polarization of the band-edge luminescence under ($\sigma^+$) excitation

$$P \equiv \frac{I(\sigma^+) - I(\sigma^-)}{I(\sigma^+) + I(\sigma^-)} \tag{1}$$

 

is therefore equal to the spin polarization of the electrons $\langle \mathbf{S} \rangle$ and is given by[13]

$$P(0)=P^*\tau_s/(\tau_s+\tau_r) , \tag{2}$$

where $\tau_s$ is the spin-lattice relaxation time of the electrons, and $\tau_r$ is the luminescence decay time. $P^*$ is the polarization which can occur in the absence of spin-lattice relaxation, and is set by the interband optical matrix elements and the degeneracy of the bands. In a GaAs quantum well where the degeneracy of light- and heavy-hole bands is raised and only the heavy-hole band is occupied, $P^*$ is unity for excitation with light propagating along the growth axis ($z$).[13]

In a magnetic field $\mathbf{B}$, perpendicular to $z$, Larmor precession of the electron spins causes a depolarization of the luminescence, or Hanle effect, according to[6,13]

$$\begin{aligned} &P(\mathbf{B})=P(0)/(1+\Omega^2\tau^2) , \\ &\Omega=|g^*|\mu_B\mathbf{B}/\hbar , \\ &\tau^{-1}=\tau_r^{-1}+\tau_s^{-1} . \end{aligned} \tag{3}$$

In the present experiments we have been able to determine $g^*$ via Eqs. (1)–(3). Note that $P(\mathbf{B})$ will have a Lorentzian shape centered at $\mathbf{B}=\mathbf{0}$ if $\tau_s$ and $\tau_r$ are independent of the field. Generally the determination of $g^*$ can be difficult because, although we expect that $\tau_r$ will be independent of the field, $\tau_s$ will increase with the field.[13] Nonetheless, provided that $P(0)$ is large (say $>0.8$), indicating that spin-lattice relaxation is slow in zero field, any increase of $\tau_s$ will in practice have a minimal effect and the depolarization will follow an essentially Lorentzian curve with height $P(0)$ and width [half-width at half maximum (HWHM)]

$$\Delta B \approx \frac{\hbar}{\mu_B|g^*|}\frac{1}{\tau_r P(0)} . \tag{4}$$

We have previously demonstrated that $P(0)$ is indeed large in quantum wells containing degenerate heavy-hole populations.[14] Thus in such samples, measurements of height and width of the Hanle depolarization (see Sec. II D), together with the luminescence decay time ($\tau_r$) in zero magnetic field (Sec. II E), give reliable values of $g^*$ using (4). The sign of $g^*$ may also be determined as described in Secs. II B and II D.

### B. Nuclear-spin effects: The sign of $g^*$

In Sec. II A we considered only effects associated with polarization $\langle \mathbf{S} \rangle$ of the electronic spins. However the contract hyperfine interaction

$$H_{\rm hf}=A\mathbf{I}\cdot\mathbf{S} , \tag{5}$$

where $A$ is a constant and $\mathbf{I}$ is the nuclear spin, allows dynamic polarization $\langle \mathbf{I} \rangle$ of the nuclear spin system via mutual electron-nuclear spin flips. In GaAs the nuclear spin system comprises all the lattice nuclei, that is, the isotopes $^{69}$Ga and $^{71}$Ga, which are 60% and 40% abundant, respectively, and $^{75}$As, which is 100% abundant. In an arbitrarily directed applied magnetic field, such a nuclear polarization provides an extra, fictitious component of magnetic field $\mathbf{B}_n$, seen only by the electron spins (Overhauser effect). Provided that the external field exceeds the internuclear dipolar fields ($\sim 1g$), both $\langle \mathbf{I} \rangle$ and $\mathbf{B}_n$ are collinear with the applied field[13] and

$$\mathbf{B}_n \propto \frac{A}{g^*\mu_B}(\langle \mathbf{S} \rangle\cdot\mathbf{B})\frac{\mathbf{B}}{|\mathbf{B}|^2} , \tag{6}$$

where $\langle \mathbf{S} \rangle$ is defined by the direction and polarization of the exciting light beam (see Fig. 1).

The magnitude of $\mathbf{B}_n$ may be large, up to several teslas in GaAs,[13] and if present can complicate the interpretation of measurements of $P(\mathbf{B})$. Even though according to (6) $\mathbf{B}_n$ is zero for applied fields exactly transverse to the incident light beam (i.e., to $\langle \mathbf{S} \rangle$), there are still residual effects of nuclear polarization on $P(\mathbf{B})$ for small applied fields, as described in Sec. II D.[13] Furthermore, it is difficult under experimental conditions to achieve the transverse geometry with sufficient precision to avoid observable finite values of $\mathbf{B}_n$.

To keep things simple, as described in Sec. II A, it is necessary to avoid nuclear polarization. This can be done by making measurements of $P$ with the exciting light beam alternated between $\sigma^+$ and $\sigma^-$ polarization on a time scale fast compared with the time for dynamic nuclear polarization ($T_{1e} \geq 1$ s)[15] but slow compared to that for electron recombination ($\tau_r \leq 10^{-9}$ s). The electronic spin $\langle \mathbf{S} \rangle$ will then follow the alternation but the buildup of nuclear polarization will be blocked. It is straightforward to alternate the incident polarization at an appropriate frequency to meet these requirements, as described in Sec. II D.

On the other hand, nuclear spin polarization and its associated field $\mathbf{B}_n$ can be exploited to give the sign of $g^*$.[13] For this the magnetic field is applied at some angle ($\sim 30°$) to the transverse direction and $P(\mathbf{B})$ is measured using a fixed polarization (say $\sigma^+$) to excite the sample. The nuclear polarization and field $\mathbf{B}_n$ will then appear. The geometry is illustrated in Fig. 1, which shows the directions of incident light beam, of $\langle \mathbf{S} \rangle$ in the case of $\sigma^+$ polarization, and of an arbitrarily directed external field $\mathbf{B}$. Referring to Eq. (6), $\mathbf{B}_n$ is collinear with $\mathbf{B}$ and, furthermore, the hyperfine constant $A$ is positive, being proportional to the electron density at the nuclear positions, and to the nuclear gyromagnetic ratio which is positive for all the natural isotopes of group-III and -V elements. Thus $\mathbf{B}_n$ augments or opposes $\mathbf{B}$ according to the sign of $\langle \mathbf{S} \rangle/g^*$. To a first approximation the effect of $\mathbf{B}_n$ is to give a Lorentzian variation of $P(\mathbf{B})$ similar to that for the purely transverse geometry specified by Eq. (4), but now centered at a finite applied field[13]

$$\mathbf{B}_0=-\mathbf{B}_n . \tag{7}$$

Thus the sign of $\mathbf{B}_n$ and hence of $g^*$ can be determined unambiguously from the sign of the displacement of the center of the Lorentzian, the angle between the applied field and the exciting beam, and the sense of the exciting polarization.

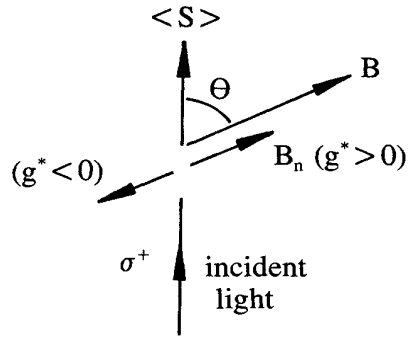


FIG. 1. The orientations of electron-spin polarization $\langle \mathbf{S} \rangle$ and nuclear field $\mathbf{B}_n$ in the two cases of $g^* > 0$ and $g^* < 0$, relative to the incident light beam (assumed $\sigma^+$ polarized). An external magnetic field $\mathbf{B}$ is applied at the angle $\theta$ to the incident beam.

### C. Samples

The samples used in these measurements have been described elsewhere in some detail.[16] They consist of series of single GaAs quantum wells of nominal widths $L_z = 5$, 10, and 20 nm separated by 31-nm $Al_{0.3}Ga_{0.7}As$ barriers grown on an $n^+$-type GaAs substrate. The wells, barriers, and a thick GaAs buffer layer immediately on top of the substrate are undoped (estimated to be approximately $10^{14}$ to $10^{15}$ cm$^{-3}$ $p$-type). Electrical bias can be applied between a transparent Indium Tin Oxide electrode on the top surface and the substrate. At flat-band bias ($\sim +0.5$ to $+1.0$ V) the quantum wells are empty and the interband spectra are dominated by hydrogenic excitons. Under reverse bias, populations of heavy holes with sheet densities up to $10^{11}$ cm$^{-2}$ accumulate in the wells, probably due to quasiresonant tunneling processes,[16] and giving absorption spectra with Fermi-edge singularities rather than hydrogenic excitons. The heavy-hole concentrations were determined from measurements of the additional Stokes shift between luminescence and luminescence excitation peaks, compared to the value for flat-band bias conditions.[16] The luminescence excitation peak energies at flat band indicated significant variation from the nominal well widths as a function of position on the wafers, which has permitted determination of $g^*$ for more values of $L_z$ than the nominal ones. The value of $L_z$ for each particular sample was determined by comparison of its flat-band heavy-hole–electron $n = 1$ absorption peak energy with those for similar samples[17] where the widths were determined by x-ray diffraction.

### D. Measurement of polarization

Figure 2 illustrates the experimental arrangement for measurement of $P(\mathbf{B})$. It is a standard cw luminescence and luminescence excitation apparatus with provision for polarization studies. The sample was mounted in superfluid helium at 1.8 K in a superconducting magnet and approximately 10 W cm$^{-2}$ of light from a cw dye laser was focused onto it along the growth axis, giving photoexcited carrier densities in the region of $10^8$ cm$^{-2}$. Backward luminescence was collected and analyzed using a 0.5-m grating spectrometer. The dye laser was tuned to the lowest-energy absorption feature of the particular quantum well under study. This was the $n = 1$ 1$s$ heavy-

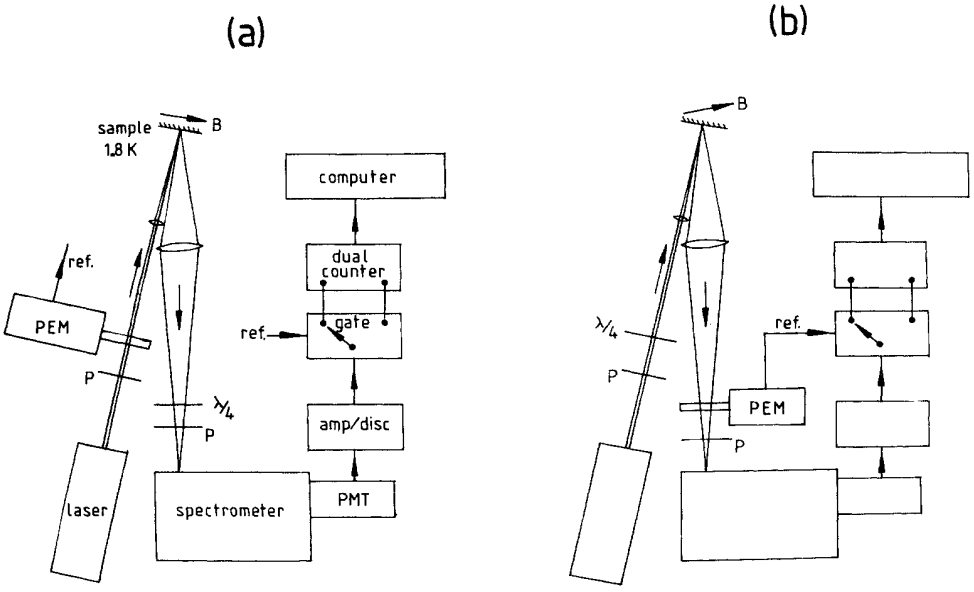


FIG. 2. Experimental arrangements for determination of luminescence polarization $P(\mathbf{B})$. In (a) the photoelastic modulator (PEM) alternates the incident laser beam between $\sigma^+$ and $\sigma^-$ polarization at 50 kHz. In (b) the sample is excited with fixed $\sigma^+$ polarization and the detected luminescence is modulated. $P$ is a linear polarizer, $\lambda/4$ a quarter wave plate, and PMT the photomultiplier tube.

hole–electron exciton peak for flat-band bias or the equivalent "Mahan" exciton peak at the Fermi edge for reverse bias.[16] The spectrometer was set to the peak of the corresponding electron–heavy-hole recombination line.

The polarization $P$ was determined using one of the two arrangements shown in Fig. 2. In Fig. 2(a) the incident laser beam is modulated between $\sigma^+$ and $\sigma^-$ polarization at 50 kHz using a photoelastic modulator (PEM), while the luminescence is passed through a fixed $\sigma^+$ analyzer (combination of $\lambda/4$ plate and linear polarizer) in front of the spectrometer slit. In this arrangement effects of nuclear-spin polarization are suppressed, as described in Sec. II B, enabling accurate measurements of $|g^*|$. In Fig. 2(b) the positions of modulator and fixed analyzer are interchanged, allowing nuclear polarization to build up so that the sign of $g^*$ may be determined. In both configurations the reference signal from the modulator operates the gate of a dual-channel pulse-counting system and an associated computer is used to obtain the value of $P$ as defined in Eq. (1).

Figure 3 illustrates typical data for $P(\mathbf{B})$, measured using the configuration of Fig. 2(a) and with the applied magnetic field perpendicular to the incident light beam. Corrections have been applied to the raw data to allow for the dark count of the photomultiplier tube and also for a background field-independent polarization signal associated with elastic scattering of nonlasing emission from the dye laser at the spectrometer wavelength. The curves in Fig. 3 are Lorentzians fitted to the experimental points. The fit is good, confirming the expectations of Sec. II A. The parameters of such fits [height $P(0)$ and width (HWHM) $\Delta B$] were used in the determination of $|g^*|$ using Eq. (4).

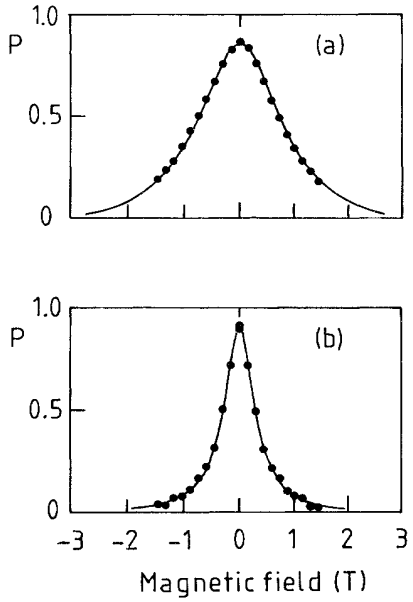


FIG. 3. Examples of Hanle depolarization curves obtained using the setup of Fig. 2(a) in a quantum-well with $L_z=9.6$ nm, containing heavy-hole densities of (a) $\sim 5\times 10^9$ cm$^{-2}$ and (b) $7\times 10^{10}$ cm$^{-2}$. The solid circles are background-corrected experimental points, and the curves are fitted Lorentzians.

Figure 4 illustrates raw uncorrected data for $P(\mathbf{B})$ for two different well widths $L_z$, obtained using the configuration of Fig. 2(b), in which nuclear polarization is important. For these measurements the external field was at 60° to the incident beam and the reverse bias was adjusted to maximize the heavy-hole concentration. In Fig. 4(a) ($L_z=9.6$ nm), $P(\mathbf{B})$ follows an approximately Lorentzian curve centered near $B_0=+0.1$ T. For this experimental geometry the positive sign of $B_0$ indicates that $\mathbf{B}_n$ opposes the external field [Eq. (7)] and that $g^*<0$ (see Fig. 1). Figure 4(b) shows measurements for a well width $L_z=5.05$ nm using the same geometry. The negative displacement of the maximum in the $P(\mathbf{B})$ curve shows that $B_n\approx+1$ T and therefore that in this case, $g^*>0$.

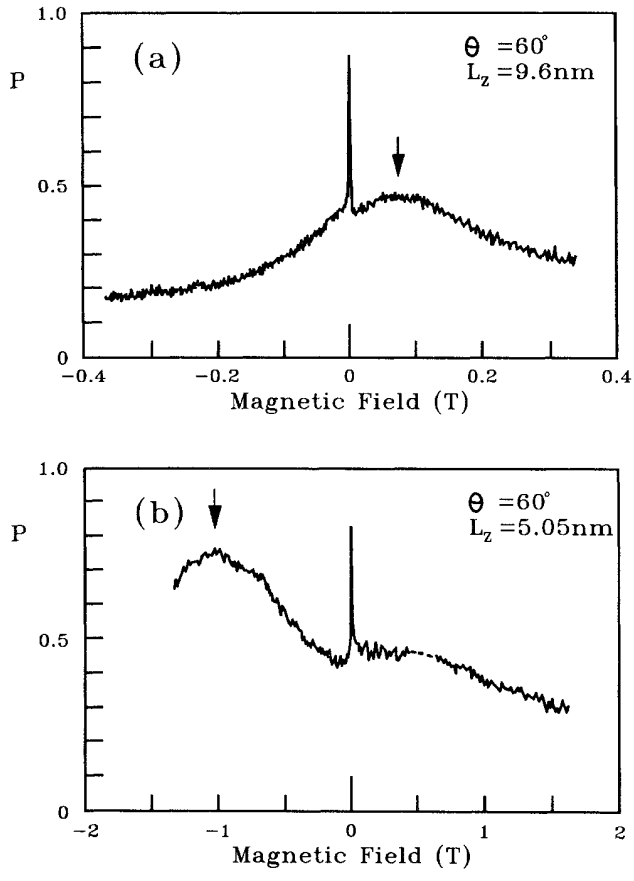


FIG. 4. Hanle depolarization curves for samples with (a) $L_z=9.6$ nm and (b) $L_z=5.05$ nm obtained using the setup of Fig. 2(b). The applied field is at an angle $\theta=60°$ to the incident beam. The scans are continuous chart recordings not corrected for background except for removal of an experimental artifact near 0.5 T. Vertical arrowheads indicate the offset center of the depolarization curve ($\mathbf{B}_0$) in each case showing that in (a) $\mathbf{B}_n=-\mathbf{B}_0\simeq-0.1$ T and therefore $g^*<0$, whereas in (b) $\mathbf{B}_n=-\mathbf{B}_0\simeq+1$ T and $g^*>0$.

The sharp peaks near $B=0$ T are not relevant to this discussion. They are associated with reorientation of the nuclear polarization at values of external field comparable to the internal nuclear dipolar fields in the sample,[13] in which regime Eq. (6) is not valid.

### E. Measurement of luminescence decay time

Luminescence decay curves were measured with a high-dynamic-range picosecond photon counting system, based upon a Delli Delti DS3/RF/SP streak camera and described in detail elsewhere.[18] The sample, mounted in liquid helium at 1.8 K, was excited at 45° to normal incidence with a train of 2-ps FWHM (full width at half maximum) pulses at 735 nm from a synchronously pumped mode-locked Styryl-8 dye laser. The luminescence was collected with wide-aperture optics and dispersed with a 0.25-m monochromator with 3-meV bandpass centered upon the $n=1$ electron to heavy-hole recombination line from each of the three quantum wells in turn for each setting of the sample bias. The overall time resolution of the system was varied in the range 20 to 50 ps to optimize signal-to-noise ratio on the recordings within the constraints of producing undistorted decay transients.

The incident laser power was kept as low as possible in order to avoid effects of exciton-exciton scattering and hot exciton populations on the luminescence decay. Under these conditions the peak photocreated carrier density was $2\times10^{9}$ cm$^{-2}$. The measured transients exhibited an initial rise on a time scale of 100 ps due to hot carrier and exciton cooling,[19] followed by an exponential decay over one to three orders of magnitude. The decay times were independent of excitation photon energy. Due to the strong variation with temperature of the radiative lifetime of excitons in quantum wells,[20] our observation of a single exponential decay indicates thermalization of the excited carrier population to the lattice temperature. Furthermore, the decays are observed over a range of instantaneous carrier densities that spans that used in measurements of $P(\mathbf{B})$ (Sec. II D). Therefore the luminescence decay times were measured in a regime of low excitation density and temperature equivalent to that used in the measurements of $P(\mathbf{B})$.

Figure 5 illustrates measured luminescence decay times $\tau_r$ and also quantum efficiencies at various applied biases for 9.6- and 21-nm wells. In these cases $\tau_r$ peaks at the flat-band condition (approximately $+1$ V) and falls sharply for small reverse bias before increasing for larger negative bias. At flat band the wells are fully depleted of carriers, so that the recombination proceeds via radiative decay of atomic excitons. The sharp fall in decay time for moderate reverse bias occurs where the Stokes shift measured in our cw measurements (Sec. II D) indicates a significant population of heavy holes in the wells (up to $10^{11}$ cm$^{-2}$). Since the quantum efficiency is only weakly dependent on bias, this reduction of decay time must be due to an enhanced radiative rate when a Fermi sea of holes is present rather than to any additional nonradiative decay process. The increase of decay time for larger bias, where the Stokes shift indicates that the wells are once more depleted, is similar to that reported previously[21,22] and ascribed to effects of electric field on electron-hole overlap. A more detailed analysis of the recombination dynamics in these samples is planned to be the subject of a separate publication[23].

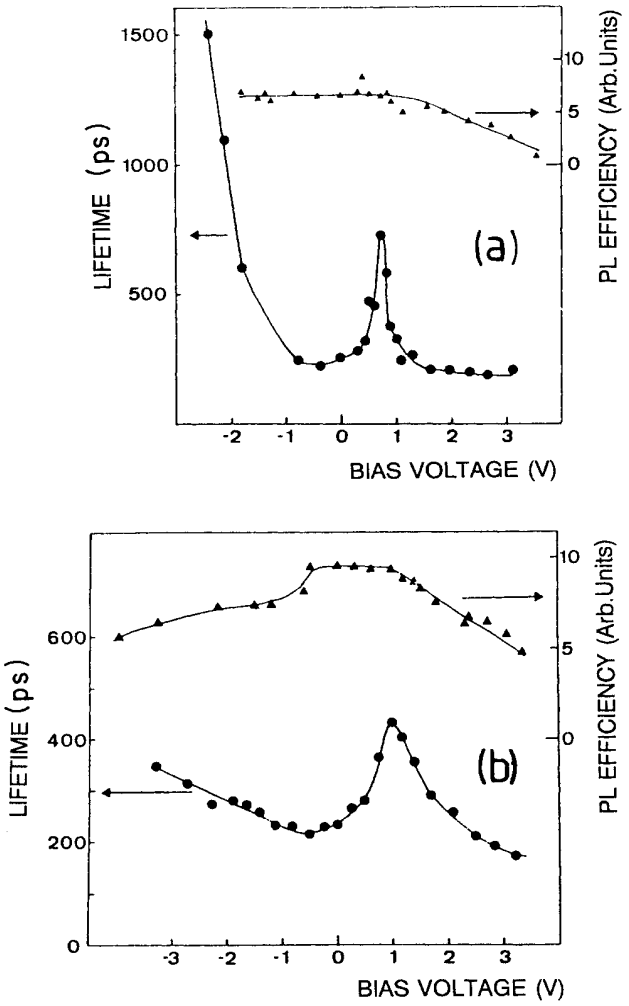


FIG. 5. Luminescence decay times and quantum efficiencies for quantum-well width (a) 20 nm and (b) 9.6 nm. For a discussion see Sec. II E.

## III. RESULTS

Figure 6 shows values of $g^*$ obtained by combining measurements of $P(\mathbf{B})$ and $\tau_r$ for different heavy-hole sheet densities for three different well widths $L_z$. The main uncertainty in the data is due to the fact that it was not possible to make measurements of the Stokes shift, and hence of hole density, at the same time as the luminescence decay time $\tau_r$. Thus the variation of $\tau_r$ with hole density is not precisely known and we have been forced to assume that the dependence of concentration on electrical bias was the same for the measurements of $\tau_r$ as for those of $P(\mathbf{B})$, where simultaneous measure-

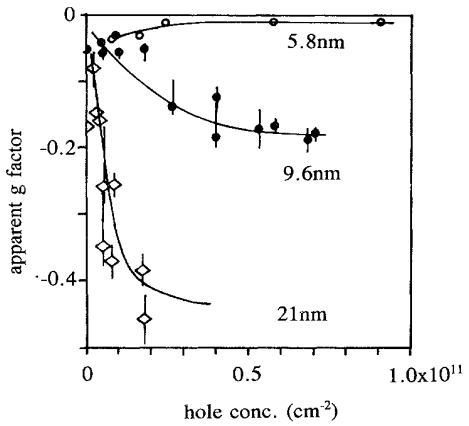


FIG. 6. Variation of the apparent $g$ factor with heavy-hole sheet density for three different quantum-well widths. The solid curves are guides for the eye.

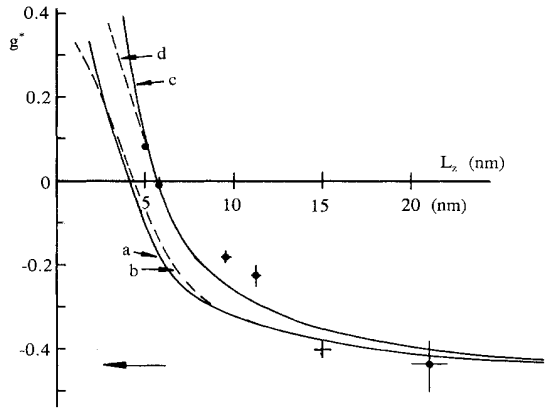


FIG. 7. Asymptotic values of $g^*$ at high concentrations of holes (see Fig. 6) for different well widths (solid circles) compared with calculations (curves). The experimental points represent the free-electron $g$ value, as argued in Sec. III. The cross is a measurement by Dobers, von Klitzing, and Weimann (Ref. 10) and the arrow indicates the bulk $g$ value for GaAs ($-0.44$).[24] Calculated curves are obtained from three-band $\mathbf{k}\cdot\mathbf{p}$ theory as described in Sec. IV. The values of nonparabolicity parameters are $K_1=0.080, K_2=-0.185$ for curves $a$ and $b$ and $K_1=0.116, K_2=-1.2$ for curves $c$ and $d$. Curves $b$ and $d$ contain allowance for electron wave-function penetration into the barriers; curves $a$ and $c$ do not.

ments of the Stokes shift were made. The associated uncertainty is quite small for well widths up to $L_z \sim 12$ nm since the variation of $\tau_r$ with bias was relatively weak [see Fig. 5(a)]. However for $L_z \sim 20$ nm, $\tau_r$ changes rapidly with bias [see Fig. 5(b)], giving rise to the large uncertainties indicated in Fig. 6. It is apparent that $g^*$ increases from a small value for low concentrations to a constant value dependent on $L_z$ for finite concentrations. For the 21-nm well the data are consistent with an asymptotic value close to that for bulk GaAs (i.e., $-0.44$), as indicated by the solid curve drawn through the points.

We interpret this behavior as follows. First, for low concentrations of heavy holes the recombination is dominated by excitonic coupling of the photocreated electron and hole. Group theory predicts that in the axial symmetry of a quantum well the $g$ factor of an exciton will be zero for magnetic fields applied perpendicular to the axis, as in this experiment, there being only a quadratic Zeeman splitting. In principle, quadratic splitting of the excitonic energy levels will give rise to a broad, non-Lorentzian depolarization curve $P(\mathbf{B})$. We have not investigated this possibility in detail but it is clear that the small apparent values of $g^*$ at low hole concentration are in general agreement with expectations. For high hole concentrations the luminescence is due to recombination of the individual photocreated electrons with holes from the degenerate Fermi sea. The electrons are initially excited at the Fermi wave vector and rapidly thermalize to the bottom of the conduction band before recombination. In these circumstances the excitonic binding becomes negligible[17] and we expect that the electron-hole exchange energy will likewise be greatly reduced. Therefore the measured $g$ value is essentially that of a free electron at the conduction-band edge.

In Fig. 7 we plot this high concentration limit of $g^*$ against well width $L_z$. The sign of $g^*$ has been determined in each case by the method outlined in Sec. II B and we find that it becomes positive for $L_z < 5.5 \pm 0.1$ nm. In principle, the free-electron $g$ value is anisotropic, so that Fig. 7 shows $g^*$ for field applied in the [110] direction in the plane perpendicular to the growth axis. However, any anisotropy will be small, probably less than our experimental uncertainty ($\mathbf{k}\cdot\mathbf{p}$ perturbation theory beyond five bands is required to describe anisotropy of $g^*$), and consequently Fig. 7 represents the electron $g$ value for all field directions. Also shown in Fig. 7 is the value obtained by Dobers, von Klitzing, and Weimann for a 15-nm $n$-type quantum well[10] in a field along the growth axis [001]. The curves in Fig. 7 represent theoretical estimates of the $g$ factor based on three-band $\mathbf{k}\cdot\mathbf{p}$ theory.

## IV. DISCUSSION

We expect that with increasing well width $g^*$ will tend to the bulk GaAs value ($-0.44$), and that for narrow wells, where the electrons spend much of their time in the barriers, $g^*$ will become positive, the value for bulk $Al_{0.3}Ga_{0.7}As$ being $\sim +0.4$.[6,24] Although this is observed experimentally, such qualitative considerations do not indicate the form of variation nor the relative importance of the barrier penetration for intermediate well widths.

In order to model the variation of $g^*$ with $L_z$, we assume that the main effect of quantum confinement is that the motion of the electrons at the lowest point in the $n=1$ subband is equivalent to that of electrons in bulk GaAs at the same energy above the band edge. The variation of $g^*$ then arises because of nonparabolicity of the

bulk conduction band. (We shall see that barrier penetration has a comparatively small effect on $g^*$.) We use for convenience three-band $\mathbf{k}\cdot\mathbf{p}$ perturbation theory as developed by Wallis for the conduction-band dispersion of bulk materials (see Palik *et al.*[5]). The dependence of $g^*$ on energy $E$ above the bottom of the conduction band to fourth order in effective-mass theory is the solution of

$$g^* = g_0^* + 4K_1 \frac{m}{m^*} \frac{E_1}{E_g} \tag{8}$$

and

$$E = E_1 + K_2 \frac{E_1^2}{E_g} , \tag{9}$$

where $g_0^*(=-0.44)$ is the $g$ value and $m^*/m$ $(=0.0667)$ is the effective-mass ratio at the bottom of the band, and $E_g(=1.519$ eV) is the band gap for GaAs.[24] These parameter values together with the spin-orbit splitting $\Delta_0(=0.341$ eV) for GaAs then fix the values of the two nonparabolicity parameters $K_1=0.080$ and $K_2=-0.85$. To compare these expressions with the experimental data for quantum wells, we replace $E$ by the measured electron confinement energy for $GaAs/Al_{0.3}Ga_{0.7}As$ quantum wells,[1] and obtain curve $a$ in Fig. 7.

To include the effect on $g^*$ of penetration of the confined electron wave function into the quantum-well barriers we use the conclusions of recent investigations of cyclotron resonance in GaAs/AlAs superlattices.[25] These suggest that the effective mass of electrons in a superlattice may be obtained by taking the mean value of $(m/m^*-1)$, the quantity calculated in $\mathbf{k}\cdot\mathbf{p}$ perturbation expansions, for the well and barrier regions weighted according to the probability of the electron being found in the well or the barrier. The values of $m^*$ required are that of an electron in the well region at the subband edge and that of an electron at the *same energy* in the barrier. In the case of the $g$ factor, the effect of barrier penetration can be estimated by taking a similar weighted mean of the quantity $(g^*/2-1)$. Curve $b$ in Fig. 7 shows the effect of such a correction for barrier penetration on curve $a$. We have used a three-band $\mathbf{k}\cdot\mathbf{p}$ perturbation calculation[13,26] to estimate values for $(g^*/2-1)$ in the $Al_xGa_{1-x}As$ barriers at the energy of the confined electrons in the GaAs wells. The appropriate weighting factors for different values of $L_z$ were obtained from calculations of electron envelope function assuming 60:40 conduction-band–valence-band energy offset. The difference between curves $a$ and $b$ in Fig. 7 is not large, justifying our rather crude estimates for the correction.

Although they show the right trend, curves $a$ and $b$ do not fit the experimental data well. In particular, they do not pass through zero at the correct value of $L_z$ (5.5 nm), which is a point that is rather precisely located by our measurements. Rogers *et al.*[1] and Singleton *et al.*[2] found that a satisfactory description of the variations of effective mass in GaAs/AlAs quantum wells could only be obtained by allowing the parameter $K_2$ to vary from that specified by the theory.[5] In curve $c$ of Fig. 7 we use their adjusted value $(-1.2)$ in Eq. (9) and adjust $K_1$ from 0.080 to 0.116 to make the calculated $g^*$ value pass through zero at $L_z=5.5$ nm. Curve $c$ is the calculation without allowance for wave-function penetration into the barriers, while curve $d$ includes it. Again the difference between these curves is small, especially for $L_z \geq 5$ nm, and each now gives a reasonable representation of the experimental data.

It is interesting that a similar fractional adjustment is required for the parameter $K_1$ (0.080 to 0.116) to achieve a satisfactory fit to $g$ factor measurements as is required for $K_2$ $(-0.85$ to $-1.2)$ to fit the effective mass. Although it is tempting to ascribe the values of $K_1$ and $K_2$ to effects of quantum confinement, it is not really surprising that the simple unadjusted three-band $\mathbf{k}\cdot\mathbf{p}$ perturbation theory (curves $a$ and $b$) fails to fit the data in view of the fact that it is an expansion about the bulk conduction-band edge. It will become increasingly inaccurate as the ratio of confinement energy to band gap increases.

We conclude, therefore, that to a first approximation at least, as with the effective mass, the $g$ factors for electrons in $GaAs/Al_xGa_{1-x}As$ quantum wells have the same values as those for electrons in the conduction band of bulk GaAs at an energy above the band edge equal to the quantum confinement energy. The effect of penetration of the electron wave functions into the barriers is rather small for $L_z \geq 5$ nm. A better theoretical treatment would take account of the modifications to the bulk conduction band induced in quantum-well systems. It seems likely that the effect of such refinement will be quite small, particularly for values of $L_z$ greater than $\sim 5$ nm, and more accurate measurements may be required to test them.

## ACKNOWLEDGMENTS

It is a pleasure to thank Dr. M. A. Brummell and Dr. R. J. Nicholas for helpful discussions.

*Present address: Physics Department, Exeter University, United Kingdom.

†Present address: Max Planck Institute, Heisenbergstrasse, Stuttgart, Germany.

[1] D. C. Rogers, J. Singleton, R. J. Nicholas, C. T. Foxon, and K. Woodbridge, Phys. Rev. B **34**, 4002 (1986).

[2] J. Singleton, R. J. Nicholas, D. C. Rogers, and C. T. B. Foson, Surf. Sci. **196**, 429 (1988).

[3] G. P. Flinn, R. T. Harley, M. J. Snelling, A. C. Tropper, and T. M. Kerr, Semicond. Sci. Technol. **5**, 533 (1990).

[4] For a preliminary report, see M. J. Snelling, G. P. Flinn, A. S. Plaut, R. T. Harley, A. C. Tropper, R. Eccleston, and C. C. Phillips, *The Electronic g-factor in GaAs/AlGaAs Quantum Wells*, International Conference on Quantum Electronics Technical Digest Series, 1990 (Optical Society of America, Washington, DC, 1990), Vol. 8, p. 367.

[5]E. D. Palik, G. S. Picus, S. Teitler, and R. F. Wallis, Phys. Rev. **122**, 475 (1961).
[6]D. J. Chadi, A. H. Clark, and R. D. Burnham, Phys. Rev. B **13**, 4466 (1976).
[7]H. W. van Kesteren, E. C. Cosman, W. A. J. A. van der Poel, and C. T. Foxon, Phys. Rev. B **41**, 5283 (1990).
[8]G. R. Johnson, A. Kana-ah, B. C. Cavenett, M. S. Skolnick, and S. J. Bass, Semicond. Sci. Technol. **2**, 182 (1987).
[9]A. S. Plaut, D. Phil. thesis, Oxford University (1988).
[10]M. Dobers, K. von Klitzing, and G. Weimann, Phys. Rev. B **38**, 5453 (1988).
[11]M. Krapf, G. Denninger, H. Pascher, G. Weimann, and W. Schlapp, Solid State Commun. **74**, 1141 (1990).
[12]See, for example, Th. Englert, D. C. Tsui, A. C. Gossard, and Ch. Uihlein, Surf. Sci. **113**, 295 (1982); F. F. Fang and P. J. Stiles, Phys. Rev. **174**, 823 (1968); R. J. Nicholas, M. A. Brummell, J. C. Portal, K. Y. Chang, A. Y. Cho, and T. P. Pearsall, Solid State Commun. **45**, 911 (1983); T. Ando and Y. Uemura, J. Phys. Soc. Jpn. **37**, 1044 (1974).
[13]See *Optical Orientation,* edited by F. Meier and B. P. Zakharchenya (North-Holland, Amsterdam, 1984) for a review of and references to all aspected of polarized opitcal excitation of bulk semiconductors.
[14]M. J. Snelling, A. S. Plaut, G. P. Flinn, A. C. Tropper, R. T. Harley, and T. M. Kerr, J. Lumin. **45**, 208 (1990).
[15]M. Krapf, G. Denninger, H. Pascher, G. Weimann, and W. Schlapp, Solid State Commun. **78**, 459 (1991).
[16]S. R. Andrews, A. S. Plaut, R. T. Harley, and T. M. Kerr, Phys. Rev. B **41**, 5040 (1990); A. S. Plaut, R. T. Harley, S. R. Andrews, and T. M. Kerr, *ibid.* **42**, 1332 (1990).
[17]J. W. Orton, P. F. Fewster, J. P. Gowers, P. Dawson, K. J. Moore, P. J. Dobson, C. J. Curling, C. T. Foxon, K. Woodbridge, G. Duggan, and H. I. Ralph, Semicond. Sci. Technol. **2**, 597 (1987).
[18]R. Eccleston and C. C. Phillips, J. Phys. E **22**, 405 (1989).
[19]J. Shah, D. Y. Oberli, D. S. Chemla, J. E. Cunningham, and J. M. Kuo, J. Lumin. **45**, 181 (1990).
[20]J. Feldmann, G. Peter, E. O. Gobel, P. Dawson, K. Moore, C. T. Foxon, and R. J. Elliott, Phys. Rev. Lett. **59**, 2337 (1987); **60**, 243(E) (1988).
[21]H.-J. Polland, L. Schultheis, J. Kuhl, E. O. Gobel, and C. W. Tu, Phys. Rev. Lett. **55**, 2610 (1987); H.-J. Polland, K. Kohler, L. Schultheis, J. Kuhl, E. O. Gobel, and C. W. Tu, Superlatt. Microstruct. **2**, 309 (1986).
[22]C. C. Phillips, R. Eccleston, and S. R. Andrews, Phys. Rev. B **40**, 9760 (1989).
[23]C. C. Phillips, R. Eccleston, S. R. Andrews, and R. T. Harley (unpublished).
[24]C. Weisbuch and C. Hermann, Phys. Rev. B **15**, 516 (1977).
[25]G. Brozak, E. A. de Andrade e Silva, L. J. Sham, F. DeRosa, P. Miceli, S. A. Schwarz, J. P. Harbison, L. T. Florez, and S. J. Allen, Jr., Phys. Rev. Lett. **64**, 471 (1990).
[26]C. Hermann and C. Weisbuch, Phys. Rev. B **15**, 823 (1977).